Inorganic Chemistry

Article

pubs.acs.org/IC

Photochemical Oxidation of a Manganese(III) Complex with Oxygen and Toluene Derivatives to Form a Manganese(V)-Oxo Complex

Jieun Jung,[†] Kei Ohkubo,[†] Katharine A. Prokop-Prigge,[‡] Heather M. Neu,[‡] David P. Goldberg,*[,‡] and Shunichi Fukuzumi*[,†,§]

[†]Department of Material and Life Science, Graduate School of Engineering, ALCA, Japan Science and Technology Agency, Osaka University, Suita, Osaka 565-0871, Japan

[‡]Department of Chemistry, The Johns Hopkins University, Baltimore, Maryland 21218, United States

[§]Department of Bioinspired Science, Ewha Womans University, Seoul 120-750, Korea

Supporting Information

ABSTRACT: Visible light photoirradiation of an oxygen-saturated benzonitrile solution of a manganese(III) corrolazine complex [$(TBP_8Cz)Mn^{III}$] (**1**): [TBP_8Cz = octakis(*p*-*tert*-butylphenyl)corrolazinato^{3-}] in the presence of toluene derivatives resulted in formation of the manganese(V)-oxo complex [$(TBP_8Cz)Mn^{V}(O)$]. The photochemical oxidation of $(TBP_8Cz)Mn^{III}$ with O_2 and hexamethylbenzene (HMB) led to the isosbestic conversion of **1** to $(TBP_8Cz)Mn^{V}(O)$, accompanied by the selective oxidation of HMB to pentamethylbenzyl alcohol (87%). The formation rate of $(TBP_8Cz)Mn^{V}(O)$ increased with methyl group substitution, from toluene, *p*-xylene, mesitylene, durene, pentamethylbenzene, up to hexamethylbenzene. Deuterium kinetic isotope effects (KIEs) were observed for toluene (KIE = 5.4) and mesitylene (KIE = 5.3). Femtosecond laser flash photolysis of $(TBP_8Cz)Mn^{III}$ revealed the formation of a tripquintet excited state, which was rapidly converted to a tripseptet excited state. The tripseptet excited state was shown to be the key, activated state that reacts with O_2 via a diffusion-limited rate constant. The data allow for a mechanism to be proposed in which the tripseptet excited state reacts with O_2 to give the putative $(TBP_8Cz)Mn^{IV}(O_2^{\bullet-})$, which then abstracts a hydrogen atom from the toluene derivatives in the rate-determining step. The mechanism of hydrogen abstraction is discussed by comparison of the reactivity with the hydrogen abstraction from the same toluene derivatives by cumylperoxyl radical. Taken together, the data suggest a new catalytic method is accessible for the selective oxidation of C−H bonds with O_2 and light, and the first evidence for catalytic oxidation of C−H bonds was obtained with 10-methyl-9,10-dihydroacridine as a substrate.

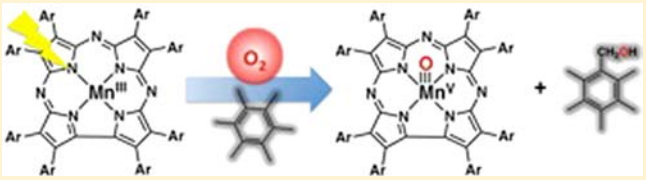

INTRODUCTION

High-valent metal-oxo species are key oxidizing intermediates in a variety of biological oxidation reactions mediated by heme and nonheme metalloenzymes involved in respiration, metabolism, and photosynthesis.[1−4] Synthetic high-valent metal-oxo complexes ($M^{(n+2)+}(O)$) are usually formed by reactions of metal complexes (M^{n+}) with two-electron oxidants such as iodosylarenes, peroxy acids, and H_2O_2 [eq 1].[5−16] However,

$$M^{n+} + H_2O_2 \rightarrow M^{(n+2)+}(O) + H_2O \quad (1)$$

enzymes such as cytochrome P450 use dioxygen (O_2) together with the addition of two electrons and two protons, which is equivalent to H_2O_2, to generate a high-valent metal-oxo species [eq 2].[1,2] On the other hand,

$$M^{n+} + O_2 + 2H^+ + 2e^- \rightarrow M^{(n+2)+}(O) + H_2O \quad (2)$$

high-valent manganese-oxo species are implicated in the water oxidation mechanism of Photosystem II, and may involve the formal two-electron oxidation of a H_2O molecule by a tetranuclear manganese complex to give high-valent Mn(O) intermediates.[4,5] Synthetic high-valent metal-oxo complexes have also been reported to be formed by two-electron oxidation of metal complexes with H_2O as the oxygen source [eq 3].[17−23]

$$M^{n+} + H_2O - 2H^+ - 2e^- \rightarrow M^{(n+2)+}(O) \quad (3)$$

There have been comparatively few reports on the formation of discrete, high-valent metal-oxo complexes using O_2.[24−26] The activation of O_2 and stabilization of high-valent metal-oxo species is challenging to carry out in a single ligand environment. Porphyrinoid ligands, and in particular corroles and corrolazines (Czs), are designed to stabilize high-valent species including high-valent metal-oxo complexes, and there are examples of $Cr^{V}(O)$ corroles generated from O_2.[27] It has recently been reported that the oxidation of a Mn^{III} corrolazine complex with O_2 in cyclohexane or toluene as solvent under visible light irradiation leads to the quantitative production of a well-characterized, isolable $Mn^{V}(O)$ complex.[28] Relatively short-lived metal-oxo species have been generated by photoinitiated homolytic axial ligand cleavage reactions with metalloporphyrins, as well as photochemical splitting of metalloporphyrin μ-oxo

Received: August 20, 2013
Published: November 12, 2013

   dx.doi.org/10.1021/ic402121j | *Inorg. Chem.* 2013, 52, 13594−13604

dimers.[29,30] However, to our knowledge the former photoinitiated reaction involving $Mn^{III}(Cz)$ is the first example of the production of a well-defined $Mn^{V}(O)$ species from O_2.

In the former study, the combined data suggested a mechanism for the generation of $Mn^{V}(O)(Cz)$ that involved solvent-assisted autoxidation, in which the solvent (cyclohexane or toluene) served as a sacrificial reductant for the activation and cleavage of a putative photactivated $Mn-O_2$ intermediate. The nature of the photoexcited state and the product(s) of solvent oxidation were not identified in this study. The proposed mechanism suggested that, perhaps under conditions involving an inert solvent, the controlled oxidation of substrates such as toluene derivatives could be mediated by $Mn^{III}(Cz)/O_2$/light.

We report herein the use of benzonitrile (PhCN) as an inert solvent for the reaction of the Mn^{III} complex [$(TBP_8Cz)Mn^{III}$: TBP_8Cz = octakis(*p-tert*-butylphenyl)corrolazinato^{3-}] with O_2 under visible light irradiation. The conversion of $(TBP_8Cz)Mn^{III}$ to $(TBP_8Cz)Mn^{V}(O)$ does not occur in PhCN in the absence of a proton/electron source, but with the addition of a series of toluene derivatives as substrates the smooth production of the $Mn^{V}(O)$ complex is observed. The concomitant oxidation of the toluene derivatives occurs with high selectivity and efficiency, leading to monohydroxylation of a benzylic position. Femtosecond laser flash photolysis (LFP) measurements resulted in the spectroscopic observation of a short-lived, O_2-reactive $(TBP_8Cz)Mn^{III}$ excited state. The LFP experiments, together with product analyses and kinetic measurements, including kinetic deuterium isotope effects, provide valuable insights into the mechanism of generation of the $Mn^{V}(O)$ complex by the photochemical oxidation of the Mn^{III} complex using O_2 as an oxygen source and toluene derivatives as the source of protons and electrons.

EXPERIMENTAL SECTION

Materials. The starting material $(TBP_8Cz)Mn^{III}$ was synthesized according to published procedures.[31] The commercially available reagents (*p*-xylene, mesitylene, durene, pentamethylbenzene, and hexamethylbenzene) were purchased with the best available purity and used without further purification. Toluene and benzonitrile (PhCN) were dried according to literature procedures[32] and distilled under Ar prior to use. The reagents 2,3,4,5,6-pentamethylbenzyl alcohol and pentamethylbenzaldehyde were also purchased with the best available purity and used without further purification from Wako Pure Chemical Industries, Ltd. and Tokyo Kasei Co., Ltd., respectively. Di-*tert*-butylperoxide was purchased from Nacalai Tesque Co., Ltd. and purified by chromatography through alumina, which removes traces of the hydroperoxide. 10-Methyl-9,10-dihydroacridine ($AcrH_2$) was prepared from 10-methylacridinium perchlorate ($AcrH^+ClO_4^-$) by reduction with $NaBH_4$ in methanol and purified by recrystallization from ethanol.[33] Cumene was purchased from Tokyo Kasei Co., Ltd. and also purified by chromatography through alumina. Deuterated toluene and mesitylene were purchased from Cambridge Isotopes in the highest purity and used as received.

Product Analysis. A PhCN solution of $(TBP_8Cz)Mn^{III}$ (5.0×10^{-4} M) was added with a microsyringe into an O_2-saturated PhCN solution containing hexamethylbenzene (2.0×10^{-2} M) as a substrate in a quartz cell. A rather large concentration of $(TBP_8Cz)Mn^{III}$ was employed to obtain detectable amounts of products by GC-MS. The mixture of the reaction was filled with O_2 and then irradiated for 24 h at room temperature, after which the solution changed from the green-brown color indicative of $(TBP_8Cz)Mn^{III}$ to the bright-green color of $(TBP_8Cz)Mn^{V}(O)$. Complete conversion of $(TBP_8Cz)Mn^{III}$ to $(TBP_8Cz)Mn^{V}(O)$ was confirmed by UV–vis spectroscopy by sampling an aliquot of the reaction mixture. An aliquot was removed and injected directly into the GC-MS for analysis. All peaks of interest were identified by comparison of retention times and coinjection with authentic samples. Compounds were quantified by comparison against a known amount of detected products using a calibration curve consisting of a plot of mole versus area. Calibration curves were prepared by using concentrations in the same range as that observed in the actual reaction mixtures. Mass spectra were recorded with a JEOL JMS-700T Tandem MS station, and the GC-MS analyses were carried out by using a Shimadzu GCMS-QP2000 gas chromatograph mass spectrometer. GC-MS conditions in these experiments were performed as follows: an initial oven temperature of 60 °C was held for 1 min and then raised 30 °C min^{-1} for 7.3 min until a temperature of 280 °C was reached, which was then held for further 10 min. This experiment was repeated three times, exhibiting error in yields within 10%.

Spectral and Kinetic Measurements. The photochemical oxidations of $(TBP_8Cz)Mn^{III}$ (7.6×10^{-6} M) with excess O_2 were examined by monitoring UV–vis spectral changes in the presence of a large excess of toluene derivatives (2.0×10^{-2} to 9.4 M) at 298 K using a Hewlett-Packard HP8453 diode array spectrophotometer under continuous irradiation of white light from a Shimadzu RF-5300PC fluorescence spectrophotometer at the same time. Typically, an aerated PhCN solution of $(TBP_8Cz)Mn^{III}$ was added with a microsyringe to an aerated PhCN solution containing the toluene derivatives in a quartz cell (total vol. 2.0 mL). Rates of oxidation reaction of $(TBP_8Cz)Mn^{III}$ to produce $(TBP_8Cz)Mn^{V}(O)$ were monitored by the decrease in the absorption band due to $(TBP_8Cz)Mn^{III}$ (λ_{max} = 695 nm, $\varepsilon_{max} = 3.51 \times 10^4$ M^{-1} cm^{-1}). The concentration of toluene derivatives were maintained in large excess as compared to [$(TBP_8Cz)Mn^{III}$] for all kinetic measurements. The limiting concentration of O_2 in PhCN solution was prepared by a mixed gas flow of O_2 and N_2. The mixed gas was controlled by using a gas mixer (Kofloc GB-3C, KOJIMA Instrument Inc.), which can mix two or more gases at a certain pressure and flow rate.

Quantum Yield Determination. A standard actinometer (potassium ferrioxalate)[34] was used for the quantum yield determination of the photochemical oxidation of $(TBP_8Cz)Mn^{III}$ with O_2 and toluene derivatives in O_2-saturated PhCN. Typically, a square quartz cuvette (10 mm i.d.), which contained an O_2-saturated PhCN solution (2.0 mL) of $(TBP_8Cz)Mn^{III}$ (7.6×10^{-6} M) and a toluene derivative was irradiated with monochromatic light of λ = 450 nm from a Shimadzu RF-5300PC fluorescence spectrophotometer. Under the conditions of actinometry experiments, the actinometer and $(TBP_8Cz)Mn^{III}$ absorbed essentially all of the incident light at λ = 450 nm. The light intensity of monochromatized light at λ = 450 nm was determined to be 3.7×10^{-8} einstein s^{-1}. The quantum yields were determined by monitoring the disappearance of absorbance at 695 nm due to $(TBP_8Cz)Mn^{III}$.

Photocatalytic Activity Measurements. The photocatalytic reactivity of $(TBP_8Cz)Mn^{III}$ (1.7×10^{-4} M) with excess of O_2 was examined by monitoring the UV–vis spectral changes in the presence of a large excess of $AcrH_2$ (0.2 M) in a quartz cell (optical path length 1 mm) using a Xe lamp (500 W) for irradiation through a transmitting glass filter (λ > 480 nm) at room temperature. In a typical experiment, $(TBP_8Cz)Mn^{III}$ (1.7×10^{-4} M) was dissolved in PhCN (0.5 mL) containing excess $AcrH_2$ (0.2 M). The solution was purged with O_2 gas for 10 min in the quartz cell, and then the reaction was initiated by irradiating the solution with a Xe lamp (500 W) transmitting through a glass filter (λ > 480 nm). The UV–vis spectra of the solution were measured using a Hewlett-Packard HP8453 diode array spectrophotometer every 1 h. The amount of 10-methyl-(9,10*H*)-acridinone (Acr=O) produced was quantified by an increase in the absorption band due to Acr=O (λ = 402 nm, $\varepsilon_{max} = 8.6 \times 10^3$ M^{-1} cm^{-1} in PhCN).

Femtosecond Laser Flash Photolysis Measurements. Measurements of transient absorption spectra in the oxidation reaction of $(TBP_8Cz)Mn^{III}$ were performed according to the following procedures. An O_2- or N_2-saturated PhCN solution containing $(TBP_8Cz)Mn^{III}$ (6.8×10^{-5} M) was excited using an ultrafast source, Integra-C (Quantronix Corp.), an optical parametric amplifier, TOPAS (Light Conversion Ltd.), and a commercially available optical detection system, Helios provided by Ultrafast Systems LLC. The source for the pump and probe pulses were derived from the fundamental output of Integra-C (λ = 786 nm, 2 mJ/pulse and fwhm = 130 fs) at a repetition rate of 1 kHz. 75% of the fundamental output of the laser was introduced into a second harmonic

dx.doi.org/10.1021/ic402121j | *Inorg. Chem.* 2013, 52, 13594–13604

Scheme 1. Formation of $(TBP_8Cz)Mn^{V}(O)$ from $(TBP_8Cz)Mn^{III}$ with O_2 and Toluene Derivatives under Photoirradiation (White Light)

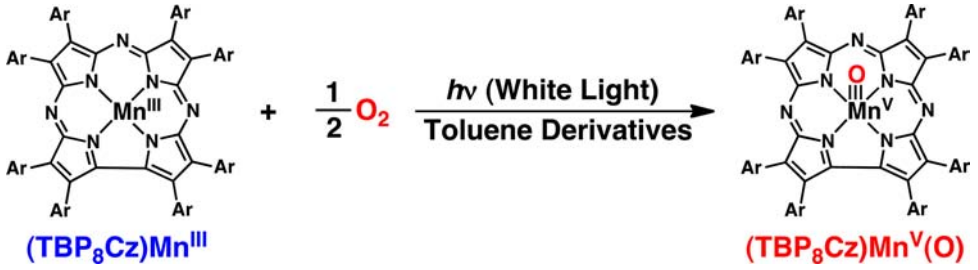

generation (SHG) unit: Apollo (Ultrafast Systems) for excitation light generation at λ = 393 nm, while the rest of the output was used for white light generation. The laser pulse was focused on a sapphire plate of 3 mm thickness and then white light continuum covering the visible region from λ = 410 to 800 nm was generated via self-phase modulation. A variable neutral density filter, an optical aperture, and a pair of polarizers were inserted in the path to generate stable white light continuum. Prior to generating the probe continuum, the laser pulse was fed to a delay line that provides an experimental time window of 3.2 ns with a maximum step resolution of 7 fs. In our experiments, a wavelength at λ = 393 nm of SHG output was irradiated at the sample cell with a spot size of 1 mm diameter where it was merged with the white probe pulse in a close angle (<10°). The probe beam after passing through the 2 mm sample cell was focused on a fiber optic cable that was connected to a CMOS spectrograph for recording the time-resolved spectra (λ = 410–800 nm). Typically, 1500 excitation pulses were averaged for 3 s to obtain the transient spectrum at a set delay time. Kinetic traces at appropriate wavelengths were assembled from the time-resolved spectral data. The decay rate of the tripquintet ($^5T_1$) obeyed the first-order kinetics given by eq 4 where A_1 is the pre-exponential factor for the absorbance changes and A_2 is the final absorbance at 530 nm

$$\Delta Abs = A_1 \exp(-k_1 t) + A_2 \quad (4)$$

and k_1 is the rate constant of the decay of the tripquintet ($^5T_1$) after irradiation. The slower decay rate of the tripseptet ($^7T_1$) also obeyed the first-order kinetics given by eq 5, where A_1 and A_2 are pre-exponential factors for the absorbance changes, A_3 is the final absorbance at 774 nm and k_2 is the rate

$$\Delta Abs = A_1 \exp(-k_1 t) + A_2 \exp(-k_2 t) + A_3 \quad (5)$$

constant of the decay of $^7T_1$. All measurements were conducted at room temperature, 298 K.

EPR Measurements. Photoirradiation of an oxygen-saturated propionitrile solution containing di-*tert*-butylperoxide (1.0 M) and cumene (1.0 M) with a 1000 W mercury lamp (Ushio-USH1005D) through an aqueous filter resulted in formation of cumylperoxyl radical (g = 2.0156).[35] The electron paramagnetic resonance (EPR) spectra were measured with a JEOL X-band spectrometer (JES-RE1XE) and recorded under nonsaturating microwave power conditions. The magnitude of modulation was chosen to optimize the resolution and the signal-to-noise (S/N) ratio of the observed spectra. The g value was calibrated by using a Mn^{2+} marker. Upon cutting off the light irradiated through a window directly, the decay of the EPR intensity was recorded with time. The decay rates were accelerated by the presence of toluene derivatives, indicating hydrogen atom transfer occurred. Rates of hydrogen atom transfer from toluene derivatives to cumylperoxyl radical were monitored by measuring the decay of the EPR signal in the presence of various concentrations of toluene derivatives in propionitrile at −80 °C. Pseudo-first-order rate constants were determined by a least-squares curve fitting procedure. The first-order plots of $\ln(I - I_\infty)$ vs time (I and I_∞ are the EPR intensity at time t and the final intensity, respectively) were linear for three or more half-lives with the correlation coefficient, ρ > 0.99. Plot of the pseudo-first-order rate constants against the substrate concentrations gave linear lines.

RESULTS AND DISCUSSION

Photochemical Oxidation of $(TBP_8Cz)Mn^{III}$ with O_2 and Toluene Derivatives. The photochemical generation of a $Mn^{V}(O)$ complex using O_2 as an oxygen source was performed by photoirradiation of an aerated PhCN solution containing a Mn^{III} complex [$(TBP_8Cz)Mn^{III}$] and toluene derivatives (Scheme 1). Monitoring this reaction by UV–vis spectroscopy revealed the transformation of $(TBP_8Cz)Mn^{III}$ (λ_{max} = 695 nm, ε_{max} = 3.51 × 10^4 M^{-1} cm^{-1}) to the $Mn^{V}(O)$ complex [$(TBP_8Cz)Mn^{V}(O)$] (λ_{max} = 634 nm, ε_{max} = 2.0 × 10^4 M^{-1} cm^{-1})[28] with isosbestic points as shown in Figure 1. No further

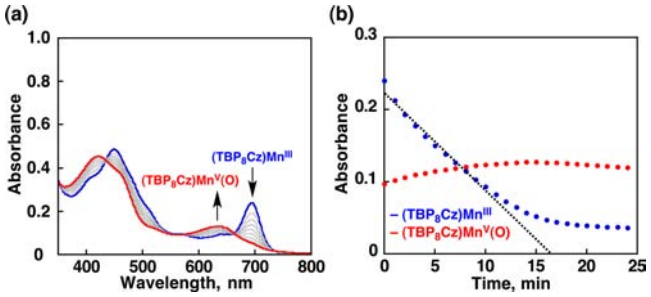

Figure 1. (a) UV–vis spectral changes and (b) time profiles of absorption changes at λ = 695 and 634 nm for the photochemical oxidation reaction of $(TBP_8Cz)Mn^{III}$ (7.6 × 10^{-6} M) under irradiation (white light) in an aerobic solution of PhCN containing hexamethylbenzene (0.08 M) as a substrate at room temperature. The dotted line is the best fit of the initial rate.

reaction of $(TBP_8Cz)Mn^{V}(O)$ with toluene occurred for another 1 h (Supporting Information, Figure S1), as expected from previous work.[28,36] No formation of $(TBP_8Cz)Mn^{V}(O)$ was observed in the absence of O_2 or toluene derivatives, indicating both toluene derivatives and O_2 are certainly required to generate $(TBP_8Cz)Mn^{V}(O)$ (Supporting Information, Figures S2 and S3).

The photochemical oxidation of $(TBP_8Cz)Mn^{III}$ with O_2 and hexamethylbenzene to produce $(TBP_8Cz)Mn^{V}(O)$ is accompanied by the oxidation of hexamethylbenzene. Analysis of the reaction mixture by GC-MS reveals the major product of oxidation to be the pentamethylbenzyl alcohol in 87% yield (based on total Mn content), along with a small amount of pentamethylbenzaldehyde (8%) (see Supporting Information, Figures S4–S5, and Table S1). Thus the oxidation of hexamethylbenzene occurs with high selectivity, and the stoichiometry of the main reaction is given by eq 6.

$$(TBP_8Cz)Mn^{III} + O_2 + C_6Me_6 \xrightarrow{h\nu} (TBP_8Cz)Mn^{V}(O) + C_6Me_5CH_2OH \quad (6)$$

dx.doi.org/10.1021/ic402121j | Inorg. Chem. 2013, 52, 13594–13604

Kinetics. Rates of formation of $(TBP_8Cz)Mn^{V}(O)$ in the photochemical oxidation of $(TBP_8Cz)Mn^{III}$ with O_2 in the air and toluene derivatives were monitored from the decay of absorbance at 695 nm due to $(TBP_8Cz)Mn^{III}$ in aerated PhCN at 298 K. The zeroth-order rate constant (k_{obs}) was determined from the initial rate in Figure 1b to avoid the decrease in the light intensity absorbed by $(TBP_8Cz)Mn^{III}$ in the course of the photochemical reaction. The k_{obs} values were derived from the initial slopes of the plots of $[(TBP_8Cz)Mn^{III}]$ vs time for the different substrates, as shown in Supporting Information, Figures S6–S11. The observed rate constants are proportional to concentrations of substrates, as shown in Figure 2 (see Supporting Information, Figure S12 for separate figures). The rates are also proportional to concentration of O_2 (Figure 3). Thus, the rate law is given by eq 7, where k_{ox} is a second-order

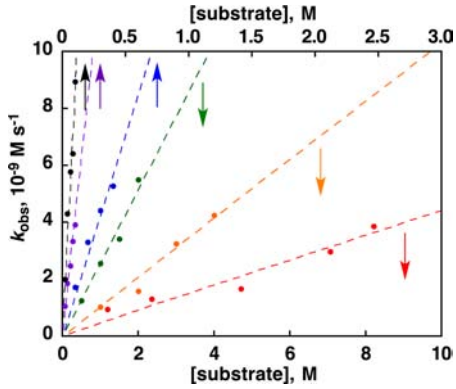

Figure 2. Plots of the observed zeroth-order rate constants (k_{obs}) of the oxidation reaction of $(TBP_8Cz)Mn^{III}$ (7.6×10^{-6} M) under irradiation (white light) of an aerated PhCN solution containing toluene (red, 1.0 to 8.2 M), *p*-xylene (orange, 1.0 to 4.0 M), mesitylene (green, 0.5 to 2.0 M), durene (blue, 0.1 to 0.4 M), pentamethylbenzene (purple, 2.0×10^{-2} to 1.0×10^{-1} M) or hexamethylbenzene (black, 2.0×10^{-2} to 1.0×10^{-1} M) as a substrate at 298 K.

$$-d[(TBP_8Cz)Mn^{III}]/dt = k_{ox}[S][O_2] \quad (7)$$

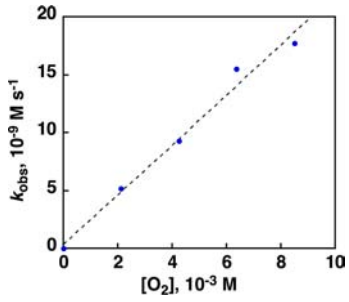

Figure 3. Plot of the observed zeroth-order rate constants (k_{obs}) for the oxidation of $(TBP_8Cz)Mn^{III}$ (7.6×10^{-6} M) with O_2 and hexamethylbenzene (0.10 M) under photoirradiation (white light) in PhCN vs the oxygen concentration ($0–8.5 \times 10^{-3}$ M)[37] at 298 K.

constant and [S] is substrate concentration. The slope of the best-fit lines for the k_{obs} values for the different substrates in Figure 2 yield first-order rate constants with respect to substrate concentration. These values can then be divided by the excess O_2 concentration (1.7×10^{-3} M) to give the second-order rate constants (k_{ox}) listed in Table 1. Interestingly, the second-order rate constants increase with an increasing number of methyl groups in the substrate. A dramatic 200-fold rate enhancement is observed in the presence of hexamethylbenzene over toluene.

Table 1. Second-Order Rate Constants for the Oxidation of $(TBP_8Cz)Mn^{III}$ (k_{ox}) by O_2 with Toluene Derivatives in Aerated PhCN at 298 K and for the Hydrogen-Atom Transfer from Toluene Derivatives to Cumylperoxyl Radicals (k'_H) in Aerated Propionitrile at 193 K

substrate	k_{ox}, M^{-1} s^{-1}	k'_H, M^{-1} s^{-1}
toluene	$(4.0 \pm 0.4) \times 10^{-7}$	$(6.5 \pm 0.2) \times 10^{-3}$
p-xylene	$(1.1 \pm 0.3) \times 10^{-7}$	$(8.3 \pm 0.3) \times 10^{-3}$
mesitylene	$(2.7 \pm 0.1) \times 10^{-6}$	$(9.2 \pm 0.4) \times 10^{-3}$
durene	$(1.2 \pm 0.4) \times 10^{-6}$	$(2.3 \pm 0.1) \times 10^{-2}$
pentamethylbenzene	$(3.6 \pm 0.1) \times 10^{-5}$	$(4.7 \pm 0.2) \times 10^{-2}$
hexamethylbenzene	$(8.0 \pm 0.2) \times 10^{-5}$	$(1.3 \pm 0.1) \times 10^{-1}$

When toluene (2.0 M) was replaced with its deuterated analogue ($C_6D_5CD_3$), the reaction rate of formation of $(TBP_8Cz)Mn^{V}(O)$ with O_2 became significantly slower as shown in Figure 4a (blue for $C_6H_5CH_3$ and red for $C_6D_5CD_3$).

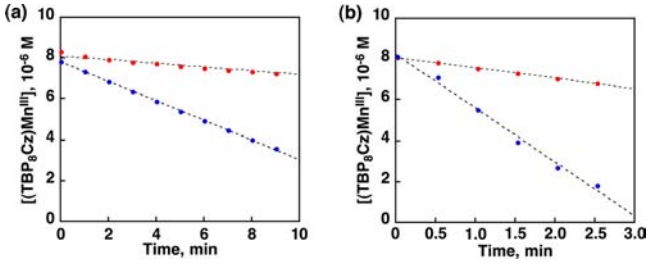

Figure 4. Time dependence of photochemical oxidation of (TBP_8Cz)-Mn^{III} (8.0×10^{-6} M) with (a) $C_6H_5CH_3$ (blue, 2.0 M), $C_6D_5CD_3$ (red, 2.0 M), (b) mesitylene (blue, 2.0 M), or mesitylene-d_{12} (red, 2.0 M) under irradiation (white light) in O_2-saturated PhCN at 298 K.

The deuterium kinetic isotope effect (KIE) for toluene was determined to be 5.4. A similar KIE was obtained for the case of mesitylene (KIE = 5.3) as shown in Figure 4b (blue for mesitylene and red for mesitylene-d_{12}). The bond-dissociation energy of the aryl C–H for benzene (109.8 kcal mol^{-1}) is over 20 kcal mol^{-1} higher than the methyl C–H for toluene (87.2 kcal mol^{-1}).[38] Thus H-atom abstraction from the methyl C–H is dramatically favored, and it is reasonable to expect that H-atom transfer from the methyl C–H occurs rather than from the aryl C–H. In fact, the photochemical reaction of benzene showed negligible formation of $(TBP_8Cz)Mn^{V}(O)$ (Supporting Information, Figure S13). The fact that the methyl group of hexamethylbenzene was oxygenated to yield pentamethylbenzyl alcohol provides additional evidence for this mechanism. Thus the KIE value corresponds to that of H-atom transfer from the methyl C–H rather than the aryl C–H. Taken together, the findings of increasing reaction rate with increasing the number of abstractable hydrogen atoms along with the observed large KIEs suggest that hydrogen-atom abstraction from the toluene derivative is directly involved in the rate-determining step for the photochemical oxidation of $(TBP_8Cz)Mn^{III}$ with O_2 and toluene derivatives.

Femtosecond Transient Absorption Measurements. To detect the photoexcited state involved in the photochemical oxidation of $(TBP_8Cz)Mn^{III}$ with O_2, the femtosecond laser flash photolysis measurements of $(TBP_8Cz)Mn^{III}$ were performed in the absence and presence of O_2 in PhCN. The Mn^{III} metal ion has a high spin d^4 ground state electronic configuration

dx.doi.org/10.1021/ic402121j | *Inorg. Chem.* 2013, 52, 13594–13604

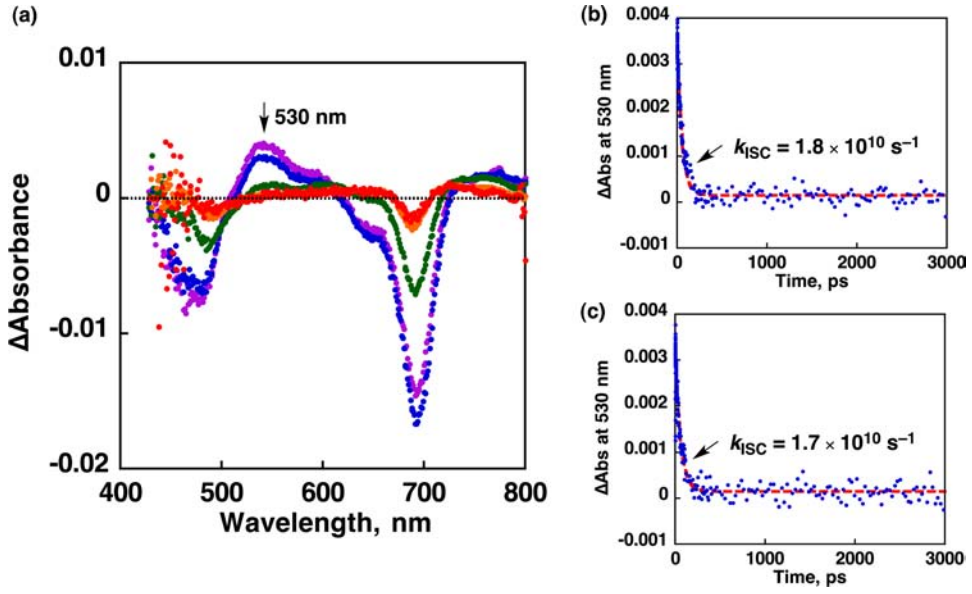

Figure 5. (a) Transient absorbance spectral changes (purple after 1 ps, blue 10 ps, green 100 ps, orange 1000 ps, and red 3000 ps) after photoexcitation of $(TBP_8Cz)Mn^{III}$ in PhCN. Time profile of the generation and decay of $[(TBP_8Cz)Mn^{III}]^*$ ($^5T_1$) at λ = 530 nm under (b) N_2 and (c) O_2. The red lines are exponential fits given in eq 4 (see Experimental Section). $A_1 = 3.3 \times 10^{-3}$, $A_2 = 1.5 \times 10^{-4}$, and $k_1 = 1.8 \times 10^{10}$ s^{-1} for (b) and $A_1 = 3.1 \times 10^{-3}$, $A_2 = 1.5 \times 10^{-4}$, and $k_1 = 1.7 \times 10^{10}$ s^{-1} for (c).

($S = 2$) with only the high energy $d_{x^2-y^2}$ orbital unoccupied in the ground state.[39] Because of the coupling between unpaired electrons of the metal with the π electrons of the corrolazine ring, the ground state of $(TBP_8Cz)Mn^{III}$ is a singquintet ($^5S_0$). Upon femtosecond laser excitation, instantaneously formed minima at λ_{min} = 450 and 695 nm can be observed as shown in Figure 5a which closely mirror the ground-state absorption spectrum (Figure 1a). A new absorption maximum at λ_{max} = 530 nm is also formed and can be assigned to the tripquintet ($^5T_1$) excited state. It is known that first row paramagnetic complexes, such as Mn^{III} complexes, undergo an extremely rapid intersystem crossing process from the singquintet ($^5S_1$) excited state to the tripquintet ($^5T_1$) excited state because of the presence of unpaired electrons.[40] In Mn^{III} porphyrins, for example, the existence of two tripmultiplet levels was suggested where a tripquintet ($^5T_1$) relaxes to a long-lived tripseptet ($^7T_1$), which requires a spin conversion to go back to the quintet ground state.[40,41] In the Mn corrolazine complex, we attribute the decay of the absorbance band at 530 nm to intersystem crossing from the $^5T_1$ state to the $^7T_1$ state, which has a small absorption band at 774 nm. The decay rate of the tripquintet ($^5T_1$) obeyed first-order kinetics with a rate constant of 1.8×10^{10} s^{-1} in deaerated PhCN (Figure 5b). The similar decay rate constant was observed in O_2-saturated PhCN (Figure 5c) showing no oxygen dependence on the rate of intersystem crossing.

The absorbance at 774 nm due to $^7T_1$ remained unchanged up to 3000 ps in deaerated PhCN (Figure 6b), whereas the absorbance decays in O_2-saturated PhCN (Figure 6c), signaling a direct reaction between the excited state and O_2. The second-order rate constant of the decay of $[(TBP_8Cz)Mn^{III}]^*$ ($^7T_1$) in the presence of O_2 was determined to be 4.9×10^9 M^{-1} s^{-1}, which is comparable to the diffusion-limited rate constant in PhCN.[42] Because the one-electron oxidation potential of $[(TBP_8Cz)Mn^{III}]^*$ ($^7T_1$) (−0.90 V vs SCE)[43−45] is more negative than the one-electron reduction potential of O_2 (−0.87 V vs SCE),[46] electron transfer from $[(TBP_8Cz)Mn^{III}]^*$ ($^7T_1$) to O_2 may occur efficiently to produce the Mn(IV)-superoxo complex, $(TBP_8Cz)Mn^{IV}(O_2^{\bullet-})$.[47]

An alternative mechanism could involve direct energy transfer from $[(TBP_8Cz)Mn^{III}]^*$ ($^7T_1$) to O_2 to produce singlet oxygen ($^1O_2$*) and the ground state $(TBP_8Cz)Mn^{III}$ ($S = 2$), which is a spin-allowed process. In the initial report on the photochemical oxidation of $(TBP_8Cz)Mn^{III}$ to $(TBP_8Cz)Mn^{V}(O)$, a significant role for singlet oxygen was ruled out by use of the $^1O_2$* trap, 9,10-dimethylanthracene.[28] However, to eliminate the possibility of $^1O_2$* as the major oxidant under inert solvent conditions as employed in the present study, we looked for the presence of $^1O_2$* by its phosphorescence spectrum (λ_{max} = 1270 nm).[37,48] The photoexcitation of $(TBP_8Cz)Mn^{III}$ in O_2-saturated C_6D_6 (PhCN could not be used because of the short lifetime of $^1O_2$) results in a much smaller phosphorescence signal at 1270 nm than that obtained by photoexcitation of C_{60} under the same conditions.[49] (see Supporting Information, Figure S14) Thus, the contribution of $^1O_2$* for the photochemical oxidation of $(TBP_8Cz)Mn^{III}$ with O_2 may be negligible as compared with an electron-transfer pathway from $[(TBP_8Cz)Mn^{III}]^*$ ($^7T_1$) to O_2.

Reaction Mechanism. Based on the photodynamics of $(TBP_8Cz)Mn^{III}$, together with the effect of added substrate and the large observed KIEs, the mechanism of photochemical oxidation of $(TBP_8Cz)Mn^{III}$ with O_2 and toluene as the substrate to produce $(TBP_8Cz)Mn^{V}(O)$ is proposed as shown in Scheme 2. Upon photoexcitation of $(TBP_8Cz)Mn^{III}$, the produced tripquintet excited state ($[(TBP_8Cz)Mn^{III}]^*$ ($^5T_1$)) is converted rapidly by intersystem crossing to the triplet excited state ($[(TBP_8Cz)Mn^{III}]^*$ ($^7T_1$)). Electron transfer from $[(TBP_8Cz)Mn^{III}]^*$ ($^7T_1$) to O_2 occurs to produce the superoxo complex $[(TBP_8Cz)Mn^{IV}(O_2^{\bullet-})]$. Hydrogen-atom transfer from toluene to $(TBP_8Cz)Mn^{IV}(O_2^{\bullet-})$ then follows as the rate-determining step, generating the hydroperoxo complex $(TBP_8Cz)Mn^{IV}(OOH)$ and benzyl radical. This reaction is most likely in competition with the back-reaction of electron transfer to regenerate the ground state $(TBP_8Cz)Mn^{III}$ and O_2. The subsequent homolytic O−O bond cleavage by benzyl radical may occur rapidly inside the reaction

dx.doi.org/10.1021/ic402121j | Inorg. Chem. 2013, 52, 13594−13604

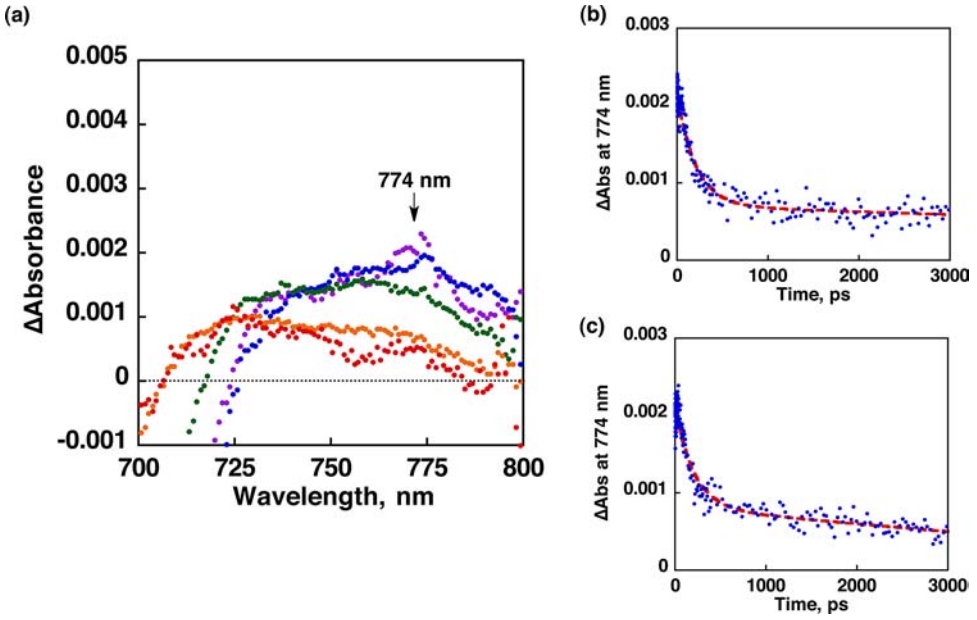

Figure 6. (a) Transient absorbance spectral changes (purple after 1 ps, blue 10 ps, green 100 ps, orange 1000 ps, and red 3000 ps) after photoexcitation of $(TBP_8Cz)Mn^{III}$ in PhCN. Decay time profiles of absorbance at 774 nm due to $[(TBP_8Cz)Mn^{III}]^*$ ($^7T_1$) (b) in N_2-saturated PhCN and (c) in O_2-saturated PhCN. Best-fit lines (red) obtained from a double-exponential kinetic model given in eq 5 (see Experimental Section). $A_1 = 1.4 \times 10^{-3}$, $A_2 = 6.7 \times 10^{-4}$, $A_3 = 3.6 \times 10^{-5}$, $k_1 = 4.8 \times 10^9$ s^{-1} and $k_2 = 6.3 \times 10^7$ s^{-1} for (b) and $A_1 = 1.0 \times 10^{-3}$, $A_2 = 1.1 \times 10^{-3}$, $A_3 = -4.5 \times 10^{-4}$, $k_1 = 5.0 \times 10^9$ s^{-1} and $k_2 = 1.1 \times 10^8$ s^{-1} for (c).

Scheme 2. Mechanism of Photochemical Oxidation of $(TBP_8Cz)Mn^{III}$ with O_2 and Toluene for Generation of $(TBP_8Cz)Mn^{V}(O)$

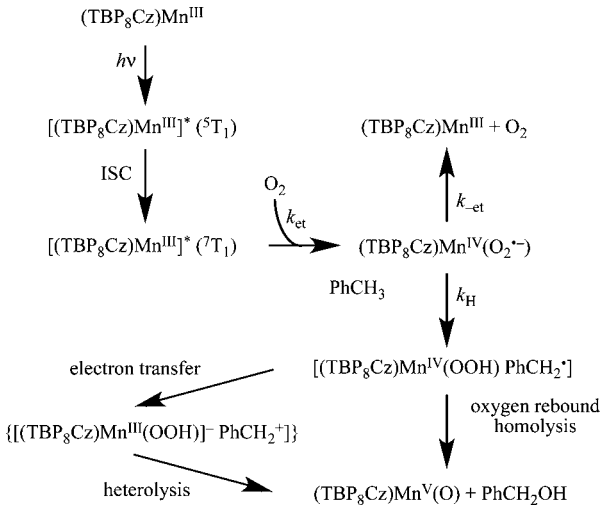

cage before the reaction of benzyl radical with O_2 to yield $(TBP_8Cz)Mn^{V}(O)$ and benzyl alcohol (an oxygen rebound pathway). Alternatively, electron transfer may occur from benzyl radical derivatives to $(TBP_8Cz)Mn^{IV}(OOH)$ to produce an ion pair $\{(TBP_8Cz)Mn^{III}(OOH)\}^-$ and benzyl cation $(PhCH_2)^+$, followed by heterolytic O−O bond cleavage to yield (TBP_8Cz)-$Mn^{V}(O)$ and benzyl alcohol derivatives. At present the homolysis vs heterolysis pathway has yet to be distinguished.

According to Scheme 2, the quantum yield of formation of $(TBP_8Cz)Mn^{V}(O)$ is given by eq 8, where Φ_0 is the quantum

$$\Phi = \Phi_0(k_H k_{et}/(k_H + k_{-et}))[S][O_2] \quad (8)$$

yield of photoinduced formation of $(TBP_8Cz)Mn^{IV}(O_2^{\bullet-})$, k_H is the rate of hydrogen-atom transfer from toluene derivatives (S) to $(TBP_8Cz)Mn^{IV}(O_2^{\bullet-})$, k_{et} is the rate constant of electron transfer from $[(TBP_8Cz)Mn^{III}]^*$ ($^7T_1$) to O_2 to produce $(TBP_8Cz)Mn^{IV}(O_2^{\bullet-})$, and k_{-et} is the back electron transfer from the $O_2^{\bullet-}$ moiety to the $(TBP_8Cz)Mn^{IV}$ moiety to regenerate $(TBP_8Cz)Mn^{III}$ and O_2. Equation 8 agrees with the empirical rate law [eq 7], in which $k_{ox} = \Phi_0(k_H k_{et}/(k_H + k_{-et}))$ In (In = light intensity absorbed by $(TBP_8Cz)Mn^{III}$).[50] Because significant KIEs were observed, as shown in Figure 4, the k_H value may be much smaller than the k_{-et} value: $k_H \ll k_{-et}$, suggesting the back electron transfer pathway is much more favored.

The mechanism in Scheme 2 is similar to O_2 activation by $[(TMC)Fe^{II}]^{2+}$ (TMC = 1,4,8,11-tetramethyl-1,4,8,11-tetraaza-cyclotetradecane) with a hydrogen donor (RH) to produce $[(TMC)Fe^{IV}(O)]^{2+}$. In this case, electron transfer from $[(TMC)$-$Fe^{II}]^{2+}$ to O_2 occurs thermally to produce $[(TMC)Fe^{III}(O_2^{\bullet-})]^{2+}$. This is followed by hydrogen transfer from RH to $[(TMC)$-$Fe^{III}(O_2^{\bullet-})]^{2+}$ to give R$^\bullet$ and $[(TMC)Fe^{III}$-$(OOH)]^{2+}$, which undergoes an oxygen rebound reaction via the homolytic O−O bond cleavage by R$^\bullet$ to yield $[(TMC)Fe^{IV}(O)]^{2+}$ and ROH.[51]

If a free radical (e.g., pentamethylbenzyl radical) were produced following hydrogen-atom transfer from a toluene derivative to $(TBP_8Cz)Mn^{IV}(O_2^{\bullet-})$, the benzyl radical should react with O_2 to produce the peroxyl radical, which may act as a chain carrier for the autoxidation of hexamethylbenzene to produce pentamethyl-benzyl hydroperoxide. The disproportionation of the peroxyl radical may yield equimolar pentamethylbenzyl alcohol and pentamethylbenzaldehyde. The fact that neither pentamethylben-zyl hydroperoxide nor pentamethylbenzaldehyde were produced and that pentamethylbenzyl alcohol was the major product, provides strong evidence for the conclusion that the rebound pathway to produce pentamethylbenzyl alcohol is faster than the rate of the reaction of pentamethylbenzyl radical with O_2. Judging from the reported rate constant of benzyl radical with O_2 (2.6×10^9 M^{-1} s^{-1})[52] to produce benzyl peroxyl radical, and the O_2

dx.doi.org/10.1021/ic402121j | Inorg. Chem. 2013, 52, 13594−13604

concentration (8.5 mM) of the reaction mixture, the lifetime of the radical is expected to be shorter than 45 ns = $(2.6 \times 10^9 \times 8.5 \times 10^{-3})^{-1}$. The lifetime of $(TBP_8Cz)Mn^{IV}(OOH)$ is also expected to be shorter than 45 ns. In such a case, it is very difficult to detect $(TBP_8Cz)Mn^{IV}(OOH)$, because this is a high energy species, which goes back to $(TBP_8Cz)Mn^{III}$, O_2, and H^+.[53,54]

Comparison of Hydrogen Transfer Reactivity. To gain deeper insight into the rate-determining hydrogen transfer from toluene derivatives to $(TBP_8Cz)Mn^{IV}(O_2^{\bullet-})$, the reactivity was compared with that of hydrogen transfer from the same toluene derivatives employed in this study to cumylperoxyl radical, which is regarded as an authentic hydrogen-transfer reaction.[35,55,56] The rates of hydrogen transfer from toluene derivatives to cumylperoxyl radical were determined by monitoring the reactions by EPR spectroscopy. Cumylperoxyl radicals were generated by photoirradiation of an aerated propionitrile solution containing di-*tert*-butylperoxide (^{t}BuO^{t}Bu) and cumene [$PhCH(CH_3)_2$] with a 1000 W Mercury lamp via a radical chain process as shown in Scheme 3.[35] The UV light irradiation of ^{t}BuO^{t}Bu results in the

Scheme 3. Generation of Cumylperoxyl Radical and Hydrogen Transfer from Toluene to $PhCMe_2OO^{\bullet}$

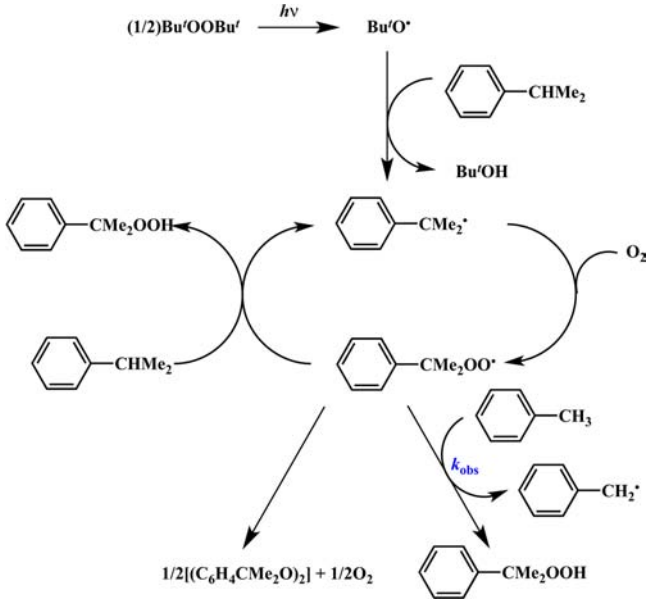

O−O bond cleavage to produce ^{t}BuO$^{\bullet}$. This radical can then readily abstract a hydrogen from cumene to generate cumyl radical [$PhC^{\bullet}(CH_3)_2$]. Rapid O_2 addition to the cumyl radical affords the cumylperoxyl radical ($PhC(CH_3)_2OO^{\bullet}$). Once generated, this autoxidation process continues until cumylperoxyl radicals decay via *ß*-scission producing acetophenone and $CH_3O^{\bullet}$.[57]

After cutting off the light, the decay rates of cumylperoxyl radical were monitored by the decrease of EPR signal intensity at g = 2.0156 in the presence of a toluene derivative in propionitrile at 193 K, as shown in Figure 7. The decay rates of cumylperoxyl radical obeyed first-order kinetics under the conditions with large excess toluene derivatives.[58] The pseudo-first-order rate constants (k'_{obs}) were linearly proportional to concentrations of toluene derivatives as shown in Figure 8. The second-order rate constants (k'_H) of the hydrogen atom transfer from toluene derivatives to cumylperoxyl radicals were determined from the slopes of linear plots in Figure 8. The k'_H values are also

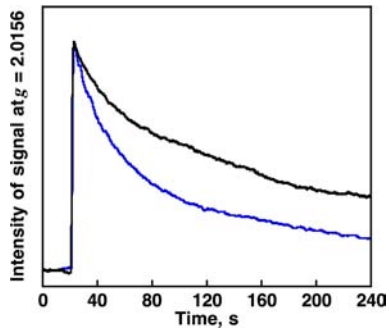

Figure 7. Time profiles of the EPR intensity change of cumylperoxyl radical in the absence (black line) and presence of toluene as a substrate (3 M, blue line) in aerated propionitrile at 193 K.

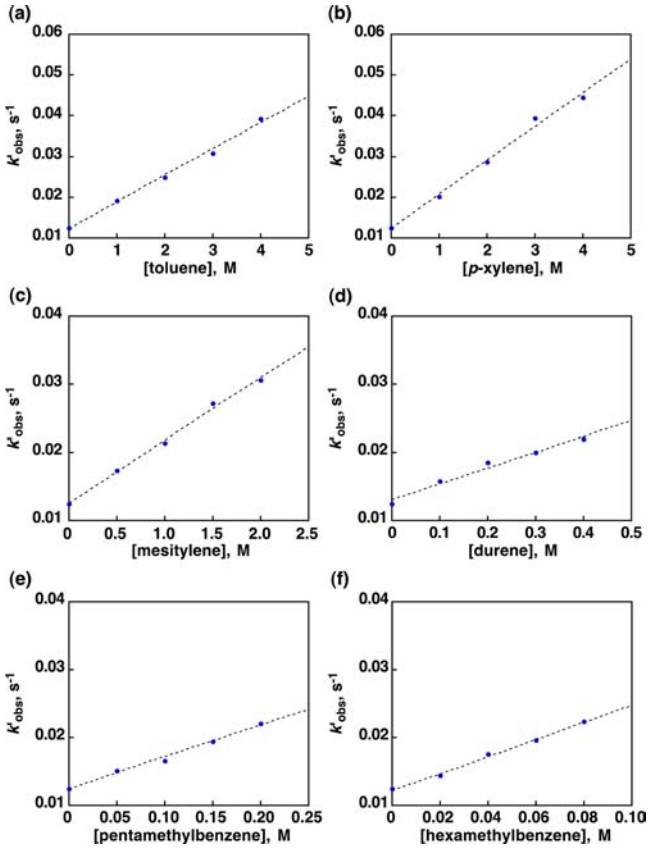

Figure 8. Plots of k'_{obs} vs concentrations of toluene derivatives for hydrogen-atom transfer from toluene derivatives to cumylperoxyl radical in aerated propionitrile at 193 K.

listed in Table 1. The decay rates of cumylperoxyl radical in the presence of a toluene derivative become faster than in the absence of the toluene derivative.

These results suggest that hydrogen-atom transfer from the toluene derivative to cumylperoxyl radical readily occurs. Figure 9 shows plots of the logarithm of the k_{ox} values of the photochemical oxidation of $(TBP_8Cz)Mn^{III}$ with O_2 in the presence of toluene derivatives and the k'_H values of hydrogen-atom transfer from toluene derivatives to cumylperoxyl radicals vs the one-electron oxidation peak potentials of the toluene derivatives (E^p_{ox}), which were reported previously.[59] There is a linear correlation between log k_{ox} and E^p_{ox} with a larger slope (3.2) than that between log k'_H and E^p_{ox} (1.7) in Figure 9. The slopes of 3.2 and 1.7 correspond to

dx.doi.org/10.1021/ic402121j | Inorg. Chem. 2013, 52, 13594−13604

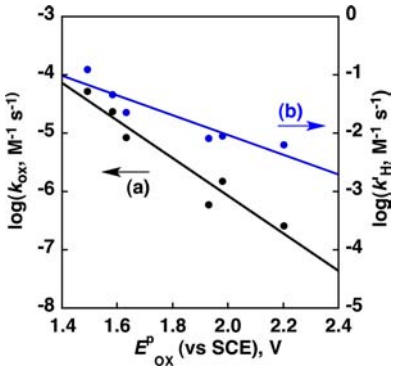

Figure 9. Plots of log k_{ox} and log k'_H against the oxidation potential (E^p_{ox}) of toluene derivatives for hydrogen-atom transfer with (a) $(TBP_8Cz)Mn^{III}$ and (b) cumylperoxyl radical.

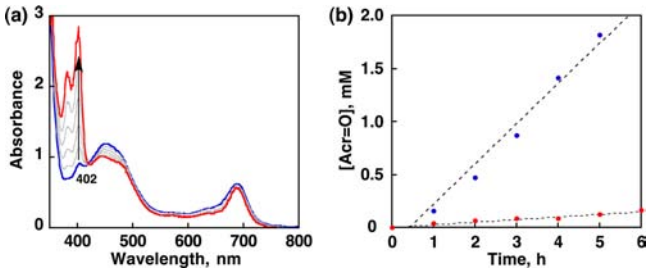

Figure 10. (a) UV−vis spectral changes and (b) time course of formed Acr=O under photoirradiation (λ > 480 nm) of an aerobic solution (0.5 mL) containing $(TBP_8Cz)Mn^{III}$ (1.7×10^{-4} M) and $AcrH_2$ (blue, 0.2 M) or $AcrD_2$ (red, 0.2 M).

19% (3.2/16.9) and 7% (1.7/26.0) of the difference in the free energy change of electron transfer, because the difference in 1 V of E_{ox} corresponds to the difference in terms of logarithm of the rate constant to be $2.3RT$ = 26.0 and 16.9 at 193 and 298 K, respectively. The k'_H value of hexamethylbenzene increases by a factor of 20 as compared with that of toluene, while the number of hydrogen atoms increases by a factor of 6. Thus, a small 3-fold "net" increase was observed in the rates of cumylperoxyl radical decay rate in the presence of hexamethylbenzene compared to its reaction with toluene. In general, the k'_H value is expected to increase with decreasing the C−H bond dissociation energies of toluene derivatives.[60] However, the C−H bond dissociation energies of toluene derivatives have been reported to be only slightly affected by the electron-donating or -withdrawing substituents.[61] The small "net" difference in the hydrogen-transfer reactivity of cumylperoxyl radical with hexamethylbenzene vs toluene results from the small change in the C−H bond dissociation energies of toluene derivatives. The larger slope (3.2) in the plot of log k_{ox} vs E^p_{ox} than the slope (1.7) in the plot of log k'_H and E^p_{ox} in Figure 9 indicates the higher degree of charge transfer in the transition state of the hydrogen-transfer reactions of $(TBP_8Cz)Mn^{IV}(O_2^{\bullet-})$ as compared with those of cumylperoxyl radical, as reported for the linear relations between logarithm of the rate constants of hydrogen-transfer reactions of triplet excited state of acetophenone derivatives and the ionization potentials of hydrogen donors.[62]

Photocatalytic Reactivity with $AcrH_2$. The photocatalytic reactivity of $(TBP_8Cz)Mn^{III}$ was examined under irradiation (white light) of a reaction solution (0.5 mL) containing $(TBP_8Cz)Mn^{III}$ (1.7×10^{-4} M) and $AcrH_2$ (0.2 M) which has a weaker C−H bond than toluene derivatives. The time course for formation of Acr=O as the product quantified by absorbance at 402 nm (λ = 402 nm, ε_{max} = 8.6×10^3 M^{-1} cm^{-1})[63] is shown in Figure 10a. The turnover number was determined to be 11 in 5 h based on the initial amount of $(TBP_8Cz)Mn^{III}$. A negligible amount of Acr=O was produced from a reaction solution without $(TBP_8Cz)Mn^{III}$ as a control experiment.

When $AcrH_2$ was replaced by the dideuterated compound $AcrD_2$, the photocatalytic reactivity dramatically decreased with a large kinetic deuterium isotope (KIE) value of 16 as shown in Figure 10b (blue for $AcrH_2$ and red for $AcrD_2$).[64] This KIE suggests that hydrogen-atom transfer from $AcrH_2$ to $(TBP_8Cz)Mn^{IV}(O_2^{\bullet-})$ is involved in the rate-determining step as seen in the case of toluene derivatives in Scheme 2. This hydrogen transfer may also proceed via electron transfer from $AcrH_2$ to $(TBP_8Cz)Mn^{IV}(O_2^{\bullet-})$, followed by rate-limiting proton transfer from $AcrH_2^{\bullet+}$ to $(TBP_8Cz)Mn^{IV}(O_2^{2-})$ to produce $AcrH^{\bullet}$ and $(TBP_8Cz)Mn^{IV}(OOH^-)$. As seen for the toluene derivatives, oxygen rebound via homolytic O−O bond

Scheme 4. Mechanism of Photocatalytic Reaction of $(TBP_8Cz)Mn^{III}$ with O_2 and $AcrH_2$

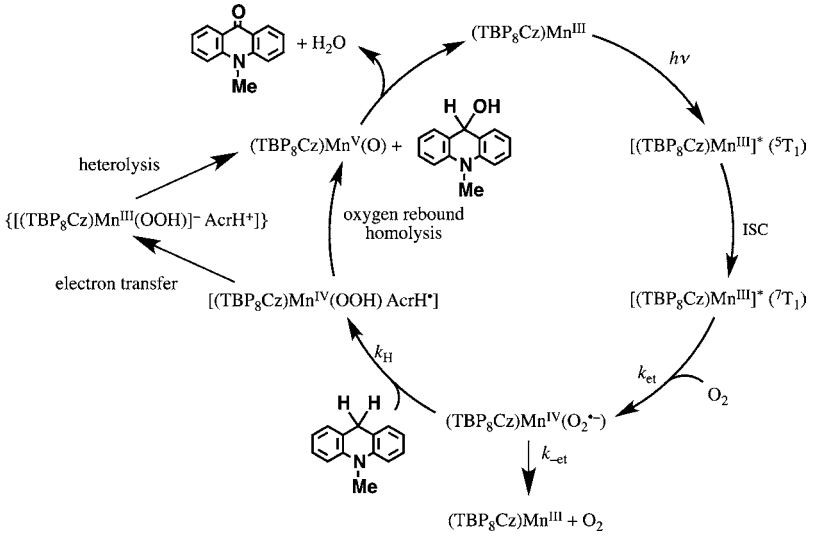

dx.doi.org/10.1021/ic402121j | Inorg. Chem. 2013, 52, 13594−13604

cleavage by AcrH$^{\bullet}$ yields $(TBP_8Cz)Mn^{V}(O)$ and AcrHOH. The electron-donating OH group in AcrHOH may make it easier to be oxidized by $(TBP_8Cz)Mn^{V}(O)$ as compared to $AcrH_2$ via electron and proton transfer, yielding Acr=O and regenerating $(TBP_8Cz)Mn^{III}$ (Scheme 4). The stoichiometry of the photocatalytic reaction is given by eq 9. The slow catalytic oxidation of $AcrH_2$ may result from the much faster back electron transfer in $(TBP_8Cz)Mn^{IV}(O_2^{\bullet-})$ as compared with the hydrogen-transfer reaction with $AcrH_2$ in Scheme 4.

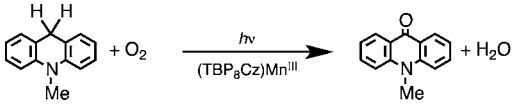

(9)

CONCLUSIONS

Photoirradiation of $(TBP_8Cz)Mn^{III}$ with O_2 and toluene derivatives in the inert solvent PhCN results in the rare formation of a high-valent manganese(V)-oxo complex with O_2 as the oxidant. At the same time, the substrate hexamethylbenzene is selectively oxidized in good yield to a single, monohydroxylated benzyl alcohol product. The photochemical mechanism was interrogated by femtosecond laser flash photolysis measurements, leading to the first direct spectroscopic observation of a novel photoexcited state ($[(TBP_8Cz)Mn^{III}]^*$ ($^7T_1$)), which was found to be responsible for the initial reaction with O_2. The LFP experiments, together with kinetic studies involving substrate dependence and KIEs, indicate that the mechanism of photochemical oxidation involves the short-lived $^7T_1$ excited state reacting with O_2 via binding and electron-transfer to produce the proposed superoxo complex $(TBP_8Cz)Mn^{IV}(O_2^{\bullet-})$. The superoxo complex then abstracts a hydrogen atom from the toluene derivatives in the rate-determining step to produce $(TBP_8Cz)Mn^{IV}(O_2H)$, followed by oxygen rebound of the resulting benzyl radical derivatives with $(TBP_8Cz)Mn^{IV}(OOH)$ to yield the corresponding benzyl alcohol derivatives and $(TBP_8Cz)Mn^{V}(O)$ (Scheme 2). The hydrogen-atom abstracting reactivity of cumylperoxyl radical was examined with the same set of toluene derivatives, and comparison of the kinetic data confirmed that H-atom abstraction was the rate-determining step for the Mn complex, and indicated that the putative $(TBP_8Cz)Mn^{IV}(O_2^{\bullet-})$ species exhibited more electrophilic character toward H-atom transfer than the cumylperoxyl radical. Our mechanistic findings suggested that catalytic oxidations should be possible with the appropriate substrate, and indeed, it was shown that carrying out the reaction with a stronger hydrogen donor such as $AcrH_2$ leads to the photocatalytic oxidation of this substrate by O_2 and $(TBP_8Cz)Mn^{III}$ as catalyst. We have thus revealed a new method for the selective oxidation of benzylic C–H bonds involving only O_2, light, and a discrete Mn^{III} complex. The mechanistic findings and accompanying model (Scheme 2) provide valuable insights into the generation of high-valent metal-oxo intermediates via O_2 activation in the presence of a hydrogen-atom (electron and proton) source.

ASSOCIATED CONTENT

Supporting Information

UV–vis spectra (Figure S1, S2, S3 and S13), GC charts (Figure S4), calibration plots for GC measurements (Figure S5), kinetic plots (Figures S6, S7, S8, S9, S10, S11, and S12), phosphorescence spectra (Figures S14), and yields of the products (Table S1). This material is available free of charge via the Internet at http://pubs.acs.org.

AUTHOR INFORMATION

Corresponding Authors

*E-mail: fukuzumi@chem.eng.osaka-u.ac.jp (S.F.).
*E-mail: dpg@jhu.edu (D.P.G.).

Notes

The authors declare no competing financial interest.

ACKNOWLEDGMENTS

This work was supported by Grants-in-Aid (No. 20108010 to S.F. and 23750014 to K.O.), the NSF (CHE0909587 and CHE121386 to D.P.G.), the NIH (GM101153 to D.P.G) by a Grant-in-Aid (20108010) and a Global COE Program (The Global Education and Research Center for Bio-Environmental Chemistry) from the Ministry of Education, Culture, Sports, Science, and Technology, Japan, and by KOSEF/MEST through the WCU Project (R31-2008-000-10010-0). K.A.P. is grateful for a Harry and Cleio Greer Fellowship.

REFERENCES

(1) (a) *Cytochrome P450: Structure, Mechanism and Biochemistry*, 3rd ed.; Ortiz de Montellano, P. R., Ed.; Kluwer: New York, 2004. (b) Rittle, J.; Green, M. T. *Science* **2010**, *330*, 933–937. (c) *Metal-Oxo and Metal-Peroxo Species in Catalytic Oxidations*; Meunier, B., Ed.; Springer-Verlag: Berlin, Germany, 2000. (d) *Cytochrome P450: Structure, Mechanism, and Biochemistry*, 3rd ed.; Ortiz de Montellano, P. R., Ed.; Kluwer Academic/Plenum Publishers: New York, 2005.

(2) (a) Sono, M.; Roach, M. P.; Coulter, E. D.; Dawson, J. H. *Chem. Rev.* **1996**, *96*, 2841–2888. (b) Groves, J. T. *Proc. Natl. Acad. Sci. U.S.A.* **2003**, *100*, 3569–3574. (c) Denisov, I. G.; Makris, T. M.; Sligar, S. G.; Schlichting, I. *Chem. Rev.* **2005**, *105*, 2253–2277. (d) Makris, T. M.; von Koenig, K.; Schlichting, I.; Sligar, S. G. J. *Inorg. Biochem.* **2006**, *100*, 507–518. (e) Meunier, B.; de Visser, S. P.; Shaik, S. *Chem. Rev.* **2004**, *104*, 3947–3980.

(3) (a) Betley, T. A.; Wu, Q.; Voorhis, T. V.; Nocera, D. G. *Inorg. Chem.* **2008**, *47*, 1849–1861. (b) Mullins, C.; Pecoraro, V. L. *Coord. Chem. Rev.* **2008**, *252*, 416–443. (c) Cady, C. W.; Crabtree, R. H.; Brudvig, G. W. *Coord. Chem. Rev.* **2008**, *252*, 444–455. (d) Photosystem II: The Light-Driven Water: Plastoquinone Oxidoreductase. In *Advances in Photosynthesis and Respiration*; Wydrzynski, T., Satoh, K., Eds.; Springer: Dordrecht, The Netherlands, 2005; Vol. *22*.

(4) (a) McEvoy, J. P.; Brudvig, G. W. *Chem. Rev.* **2006**, *106*, 4455–4483. (b) Betley, T. A.; Wu, Q.; Van Voorhis, T.; Nocera, D. G. *Inorg. Chem.* **2008**, *47*, 1849–1861. (c) Umena, Y.; Kawakami, K.; Shen, J. R.; Kamiya, N. *Nature* **2011**, *473*, 55–60. (d) Barber, J. *Inorg. Chem.* **2008**, *47*, 1700–1710.

(5) (a) Meunier, B. *Chem. Rev.* **1992**, *92*, 1411–1456. (b) Mansuy, D. *Coord. Chem. Rev.* **1993**, *125*, 129–142. (c) Groves, J. T. In *Cytochrome P450: Structure, Mechanism, and Biochemistry*, 3rd ed.; Ortiz de Montellano, P. R., Ed.; Kluwer Academic/Plenum Publishers: New York, 2005; pp 1–43. (d) Groves, J. T.; Lee, J.; Marla, S. S. *J. Am. Chem. Soc.* **1997**, *119*, 6269–6273. (e) Jin, N.; Groves, J. T. *J. Am. Chem. Soc.* **1999**, *121*, 2923–2924.

(6) (a) Nam, W. *Acc. Chem. Res.* **2007**, *40*, 465–465. (b) Nam, W. In *Comprehensive Coordination Chemistry II: From Biology to Nanotechnology*; Que, L., Jr., Tolman, W. T., Eds.; Elsevier Ltd.: Oxford, U.K., 2004; Vol. *8*, pp 281–307.

(7) (a) Martinho, M.; Blain, G.; Banse, F. *Dalton Trans.* **2010**, *39*, 1630–1634. (b) Hong, S.; Lee, Y.-M.; Shin, W.; Fukuzumi, S.; Nam, W. *J. Am. Chem. Soc.* **2009**, *131*, 13910–13911. (c) Thibon, A.; England, J.; Martinho, M.; Young, V. G., Jr.; Frisch, J. R.; Guillot, R.; Girerd, J.-J.; Munck, E.; Que, L., Jr.; Banse, F. *Angew. Chem., Int. Ed.* **2008**, *47*, 7064–7067.

(8) (a) Fujii, H. *Coord. Chem. Rev.* **2002**, *226*, 51–60. (b) McLain, J. L.; Lee, J.; Groves, J. T. In *Biomimetic Oxidations Catalyzed by Transition Metal Complexes*; Meunier, B., Ed.; Imperial College Press: London, U.K., 2000; pp 91–169. (c) Watanabe, Y. In *The Porphyrin*

Handbook, Vol. *4*; Kadish, K. M., Smith, K. M., Guilard, R., Eds.; Academic: New York, 2000; Vol. *30*, pp 97−117.
(9) (a) Sawada, Y.; Matsumoto, K.; Katsuki, T. *Angew. Chem., Int. Ed.* **2007**, *46*, 4559−4561. (b) Fujita, M.; Costas, M.; Que, L., Jr. *J. Am. Chem. Soc.* **2003**, *125*, 9912−9913.
(10) (a) Battioni, P.; Renaud, J. P.; Bartoli, J. F.; Reinaartiles, M.; Fort, M.; Mansuy, D. *J. Am. Chem. Soc.* **1988**, *110*, 8462−8470. (b) Bernadou, J.; Fabiano, A.-S.; Robert, A.; Meunier, B. *J. Am. Chem. Soc.* **1994**, *116*, 9375−9376.
(11) (a) Jin, N.; Bourassa, J. L.; Tizio, S. C.; Groves, J. T. *Angew. Chem., Int. Ed.* **2000**, *39*, 3849−3851. (b) Nam, W.; Kim, I.; Lim, M. H.; Choi, H. J.; Lee, J. S.; Jang, H. G. *Chem.—Eur. J.* **2002**, *8*, 2067−2071. (c) Zhang, R.; Newcomb, M. *J. Am. Chem. Soc.* **2003**, *125*, 12418−12419. (d) Zhang, R.; Horner, J. H.; Newcomb, M. *J. Am. Chem. Soc.* **2005**, *127*, 6573−6582. (e) Shimazaki, Y.; Nagano, T.; Takesue, H.; Ye, B.-H.; Tani, F.; Naruta, Y. *Angew. Chem., Int. Ed.* **2004**, *43*, 98−100.
(12) McLain, J. L.; Lee, J.; Groves, J. T. In *Biomimetic Oxidations Catalyzed by Transition Metal Complexes*; Meunier, B., Ed.; Imperial College Press: London, U.K., 2000; pp 91−169.
(13) Gross, Z.; Golubkov, G.; Simkhovich, L. *Angew. Chem., Int. Ed.* **2000**, *39*, 4045−4047.
(14) (a) Nam, W.; Jin, S. W.; Lim, M. H.; Ryu, J. Y.; Kim, C. *Inorg. Chem.* **2002**, *41*, 3647−3652. (b) Nam, W.; Kim, I.; Lim, M. H.; Choi, H. J.; Lee, J. S.; Jang, H. G. *Chem.−Eur. J.* **2002**, *8*, 2067−2071. (c) Fukuzumi, S.; Kishi, T.; Kotani, H.; Lee, Y.-M.; Nam, W. *Nat. Chem.* **2011**, *3*, 38−41.
(15) (a) Reginato, G.; Di Bari, L.; Salvadori, P.; Guilard, R. *Eur. J. Org. Chem.* **2000**, 1165−1171. (b) Battioni, P.; Cardin, E.; Louloudi, M.; Schollhorn, B.; Spyroulias, G. A.; Mansuy, D.; Traylor, T. G. *Chem. Commun.* **1996**, 2037−2038. (c) Nishiyama, H.; Shimada, T.; Itoh, H.; Sugiyama, H.; Motoyama, Y. *Chem. Commun.* **1997**, 1863−1864.
(16) Liu, H. Y.; Lai, T. S.; Yeung, L. L.; Chang, C. K. *Org. Lett.* **2003**, *5*, 617−620.
(17) (a) Low, D. W.; Winkler, J. R.; Gray, H. B. *J. Am. Chem. Soc.* **1996**, *118*, 117−120. (b) Berglund, J.; Pascher, T.; Winkler, J. R.; Gray, H. B. *J. Am. Chem. Soc.* **1997**, *119*, 2464−2469.
(18) (a) Hirai, Y.; Kojima, T.; Mizutani, Y.; Shiota, Y.; Yoshizawa, K.; Fukuzumi, S. *Angew. Chem., Int. Ed.* **2008**, *47*, 5772−5776. (b) Kojima, T.; Hirai, Y.; Ikemura, K.; Ogura, T.; Shiota, Y.; Yoshizawa, K.; Fukuzumi, S. *Angew. Chem., Int. Ed.* **2010**, *49*, 8449−8453. (c) Sawant, S. C.; Wu, X.; Cho, J.; Cho, K.-B.; Kim, S. H.; Seo, M. S.; Lee, Y.-M.; Kubo, M.; Ogura, T.; Shaik, S.; Nam, W. *Angew. Chem., Int. Ed.* **2010**, *49*, 8190−8194. (d) Kojima, T.; Nakayama, K.; Ikemura, K.; Ogura, T.; Fukuzumi, S. *J. Am. Chem. Soc.* **2011**, *133*, 11692−11700.
(19) (a) Bozoglian, F.; Romain, S.; Erten, M. Z.; Todorova, T. K.; Sens, C.; Mola, J.; Rodríguez, M.; Romero, I.; Benet-Buchholz, J.; Fontrodona, X.; Cramer, C. J.; Gagliardi, L.; Llobet, A. *J. Am. Chem. Soc.* **2009**, *131*, 15176−15187. (b) Sartorel, A.; Miró, P.; Salvadori, E.; Romain, S.; Carrano, M.; Scorrano, G.; Valentin, M. D.; Llobet, A.; Bonchio, M. *J. Am. Chem. Soc.* **2009**, *131*, 16051−16053.
(20) (a) Kotani, H.; Suenobu, T.; Lee, Y.-M.; Nam, W.; Fukuzumi, S. *J. Am. Chem. Soc.* **2011**, *133*, 3249−3251. (b) Kalita, D.; Radaram, B.; Brooks, B.; Kannam, P. P.; Zhao, X. *ChemCatChem* **2011**, *3*, 571−573. (c) Li, F.; Yu, M.; Jiang, Y.; Huang, F.; Li, Y.; Zhang, B.; Sun, L. *Chem. Commun.* **2011**, *47*, 8949−8951.
(21) Sartorel, A.; Carraro, M.; Scorrano, G.; Zorzi, R. D.; Geremia, S.; McDaniel, N. D.; Bernhard, S.; Bonchio, M. *J. Am. Chem. Soc.* **2008**, *130*, 5006−5007.
(22) (a) Geletii, Y. V.; Huang, Z.; Hou, Y.; Musaev, D. G.; Lian, T.; Hill, C. L. *J. Am. Chem. Soc.* **2009**, *131*, 7522−7523. (b) Besson, C.; Huang, Z.; Geletii, Y. V.; Lense, S.; Hardcastle, K. I.; Musaev, D. G.; Lian, T.; Proust, A.; Hill, C. L. *Chem. Commun.* **2010**, *46*, 2784−2786.
(23) (a) Moyer, B. A.; Thompson, M. S.; Meyer, T. J. *J. Am. Chem. Soc.* **1980**, *102*, 2310−2312. (b) Moyer, B. A.; Meyer, T. J. *Inorg. Chem.* **1981**, *20*, 436−444. (c) Che, C.-M.; Yam, V. W.-W.; Mak, T. C. W. *J. Am. Chem. Soc.* **1990**, *112*, 2284−2291. (d) Szczepura, L. F.; Maricich, S. M.; See, R. F.; Churchill, M. R.; Takeuchi, K. J. *Inorg. Chem.* **1995**, *34*, 4198−4205. (e) Che, C.-M.; Cheng, K.-W.; Chan, M. C. W.; Lau, T.-C.; Mak, C.-K. *J. Org. Chem.* **2000**, *65*, 7996−8000. (f) Meyer, T. J.; Huynh, M. H. V. *Inorg. Chem.* **2003**, *42*, 8140−8160. (g) Dhuri, S. N.; Seo, M. S.; Lee, Y.-M.; Hirao, H.; Wang, Y.; Nam, W.; Shaik, S. *Angew. Chem., Int. Ed.* **2008**, *47*, 3356−3359.
(24) (a) Tabushi, I. *Coord. Chem. Rev.* **1988**, *86*, 1−42. (b) Fukuzumi, S.; Mochizuki, S.; Tanaka, T. *Isr. J. Chem.* **1988**, *28*, 29−36.
(25) (a) Hong, S.; Lee, Y.-M.; Shin, W.; Fukuzumi, S.; Nam, W. *J. Am. Chem. Soc.* **2009**, *131*, 13910−13911. (b) Lee, Y.-M.; Hong, S.; Morimoto, Y.; Shin, W.; Fukuzumi, S.; Nam, W. *J. Am. Chem. Soc.* **2010**, *132*, 10668−10670.
(26) (a) O'Reilly, M. E.; Del Castillo, T. J.; Falkowski, J. M.; Ramachandran, V.; Pati, M.; Correia, M. C.; Abboud, K. A.; Dalal, N. S.; Richardson, D. E.; Veige, A. S. *J. Am. Chem. Soc.* **2011**, *133*, 13661−13673. (b) Egorova, O. A.; Tsay, O. G.; Khatua, S.; Huh, J. O.; Churchill, D. G. *Inorg. Chem.* **2009**, *48*, 4634−4636.
(27) (a) Meier-Callahan, A. E.; Gray, H. B.; Gross, Z. *Inorg. Chem.* **2000**, *39*, 3605−3607. (b) Meier-Callahan, A. E.; Di Bilio, A. J.; Simkhovich, L.; Mahammed, A.; Goldberg, I.; Gray, H. B.; Gross, Z. *Inorg. Chem.* **2001**, *40*, 6788−6793. (c) Mahammed, A.; Gray, H. B.; Meier-Callahan, A. E.; Gross, Z. *J. Am. Chem. Soc.* **2003**, *125*, 1162−1163. (d) Egorova, O. A.; Tsay, O. G.; Khatua, S.; Meka, B.; Maiti, N.; Kim, M. K.; Kwon, S. J.; Huh, J. O.; Bucella, D.; Kang, S. O.; Kwak, J.; Churchill, D. G. *Inorg. Chem.* **2010**, *49*, 502−512.
(28) Prokop, K. A.; Goldberg, D. P. *J. Am. Chem. Soc.* **2012**, *134*, 8014−8017.
(29) (a) Rosenthal, J.; Luckett, T. D.; Hodgkiss, J. M.; Nocera, D. G. *J. Am. Chem. Soc.* **2006**, *128*, 6546−6547. (b) Pistorio, B. J.; Chang, C. J.; Nocera, D. G. *J. Am. Chem. Soc.* **2002**, *124*, 7884−7885. (c) Harischandra, D. N.; Lowery, G.; Zhang, R.; Newcomb, M. *Org. Lett.* **2009**, *11*, 2089−2092. (d) Vanover, E.; Huang, Y.; Xu, L. B.; Newcomb, M.; Zhang, R. *Org. Lett.* **2010**, *12*, 2246−2249. (e) Peterson, M. W.; Rivers, D. S.; Richman, R. M. *J. Am. Chem. Soc.* **1985**, *107*, 2907−2915. (f) For a closely related nonporphyrin Fe−O−Fe complex, see: Ghosh, A.; de Oliveira, F. T.; Yano, T.; Nishioka, T.; Beach, E. S.; Kinoshita, I.; Münck, E.; Ryabov, A. D.; Horwitz, C. P.; Collins, T. J. *J. Am. Chem. Soc.* **2005**, *127*, 2505−2513.
(30) (a) Suslick, K. S.; Watson, R. A. *New J. Chem.* **1992**, *16*, 633−642. (b) Maldotti, A.; Amadelli, R.; Bartocci, C.; Carassiti, V.; Polo, E.; Varani, G. *Coord. Chem. Rev.* **1993**, *125*, 143−154. (c) Maldotti, A.; Bartocci, C.; Varani, G.; Molinari, A.; Battioni, P.; Mansuy, D. *Inorg. Chem.* **1996**, *35*, 1126−1131. (d) Maldotti, A.; Andreotti, L.; Molinari, A.; Carassiti, V. *J. Biol. Inorg. Chem.* **1999**, *4*, 154−161.
(31) (a) Lansky, D. E.; Mandimutsira, B.; Ramdhanie, B.; Clausen, M.; Penner-Hahn, J.; Zvyagin, S. A.; Telser, J.; Krzystek, J.; Zhan, R.; Ou, Z.; Kadish, K. M.; Zakharov, L.; Rheingold, A. L.; Goldberg, D. P. *Inorg. Chem.* **2005**, *44*, 4485−4498. (b) Ramdhanie, B.; Stern, C. L.; Goldberg, D. P. *J. Am. Chem. Soc.* **2001**, *123*, 9447−9448. (c) Mandimutsira, B. S.; Ramdhanie, B.; Todd, R. C.; Wang, H. L.; Zareba, A. A.; Czernuszewicz, R. S.; Goldberg, D. P. *J. Am. Chem. Soc.* **2002**, *124*, 15170−15171.
(32) *Purification of Laboratory Chemicals*; Armarego, W. L. F., Perrin, D. D., Eds.; Pergamon Press: Oxford, U.K., 1997.
(33) Fukuzumi, S.; Ohkubo, K.; Tokuda, Y.; Suenobu, T. *J. Am. Chem. Soc.* **2000**, *122*, 4286−4294.
(34) Hatchard, C. G.; Parker, C. A. *Proc. R. Soc. London, Ser. A* **1956**, *235*, 518−536.
(35) (a) Fukuzumi, S.; Shimoosako, K.; Suenobu, T.; Watanabe, Y. *J. Am. Chem. Soc.* **2003**, *125*, 9074−9082. (b) Matsumoto, T.; Ohkubo, K.; Honda, K.; Yazawa, A.; Furutachi, H.; Fujinami, S.; Fukuzumi, S.; Suzuki, M. *J. Am. Chem. Soc.* **2009**, *131*, 9258−9267. (c) Osako, T.; Ohkubo, K.; Taki, M.; Tachi, Y.; Fukuzumi, S.; Itoh, S. *J. Am. Chem. Soc.* **2003**, *125*, 11027−11033. (d) Ohkubo, K.; Moro-oka, Y.; Fukuzumi, S. *Org. Biomol. Chem.* **2006**, *4*, 999−1001. (e) Nakanishi, I.; Miyazaki, K.; Shimada, T.; Ohkubo, K.; Urano, S.; Ikota, N.; Ozawa, T.; Fukuzumi, S.; Fukuhara, K. *J. Phys. Chem. A* **2002**, *106*, 11123−11126. (f) Nakanishi, I.; Uto, Y.; Ohkubo, K.; Ozawa, T.; Fukuhara, K.; Fukuzumi, S.; Nagasawa, H.; Hori, H.; Ikota, N. *Org. Biomol. Chem.* **2003**, *1*, 1452−1454.

(36) (a) Lansky, D. E.; Goldberg, D. P. *Inorg. Chem.* **2006**, *45*, 5119−5125. (b) Prokop, K. A.; Visser, S. P.; Goldberg, D. P. *Angew. Chem., Int. Ed.* **2010**, *49*, 5091−5095.
(37) Fukuzumi, S.; Ohkubo, K.; Chen, Y.; Pandey, R. K.; Zhan, R.; Shao, J.; Kadish, K. M. *J. Phys. Chem. A* **2002**, *106*, 5105−5113.
(38) Berkowitz, J.; Ellison, C. B.; Gutman, D. *J. Phys. Chem.* **1994**, *98*, 2744−2765.
(39) (a) Rodriguez, J.; Holten, D. *J. Chem. Phys.* **1989**, *91*, 3525−3531. (b) Humphrey, J. L.; Kuciauskas, D. *J. Am. Chem. Soc.* **2006**, *128*, 3902−3903.
(40) (a) Yan, X.; Kirmaier, C.; Holten, D. *Inorg. Chem.* **1986**, *25*, 4774−4777. (b) Gonçalves, P, J.; De Boni, L.; Borissevitch, I. E.; Zílio, S. C. *J. Phys. Chem. A* **2008**, *112*, 6522−6526.
(41) Krokos, E.; Spänig, F.; Ruppert, M.; Hirsch, A.; Guldi, D. M. *Chem.−Eur. J.* **2012**, *18*, 1328−1341.
(42) (a) Fukuzumi, S.; Suenobu, T.; Patz, M.; Hirasaka, T.; Itoh, S.; Fujitsuka, M.; Ito, O. *J. Am. Chem. Soc.* **1998**, *120*, 8060−8068. (b) Kawashima, Y.; Ohkubo, K.; Fukuzumi, S. *J. Phys. Chem. A* **2013**, *117*, 6737−6743.
(43) The one-electron oxidation potential of $[(TBP_8Cz)Mn^{III}]^*$ ($^7T_1$) is estimated by subtracting the $^7T_1$ excited state energy (1.59 eV)[44] from the one-electron oxidation potential of the ground state.[45]
(44) The $^7T_1$ excited state energy was taken from the value of Mn^{III}TPP; see: Brookfieldh, R. L.; Llula, E.; Harriman. *J. Chem. Soc., Faraday Trans. 2* **1985**, *81*, 1837−1848.
(45) Fukuzumi, S.; Kotani, H.; Prokop, K. A.; Goldberg, D. P. *J. Am. Chem. Soc.* **2011**, *133*, 1859−1869.
(46) (a) Sawyer, D. T.; Chiericato, G., Jr.; Angelis, C. T.; Nanni, E. J., Jr.; Tsuchiya, T. *Anal. Chem.* **1982**, *54*, 1720−1724. (b) Kawashima, T.; Ohkubo, K.; Fukuzumi, S. *Phys. Chem. Chem. Phys.* **2011**, *13*, 3344−3352. (c) Fukuzumi, S.; Fujita, S.; Suenobu, T.; Yamada, H.; Imahori, H.; Araki, Y.; Ito, O. *J. Phys. Chem. A* **2002**, *106*, 1241−1247.
(47) The binding of $O_2^{\bullet-}$ to $[(TBP_8Cz)Mn^{IV}]^+$ may facilitate the electron-transfer reaction because the electron-transfer product is more stabilized thermodynamically.
(48) (a) Fukuzumi, S.; Ohkubo, K.; Zheng, X.; Chen, Y.; Pandey, R. K.; Zhan, R.; Kadish, K. M. *J. Phys. Chem. B* **2008**, *112*, 2738−2746. (b) Tanaka, M.; Ohkubo, K.; Fukuzumi, S. *J. Phys. Chem. A* **2006**, *110*, 11214−11218.
(49) (a) Araki, Y.; Dobrowolski, D. C.; Goyne, T. E.; Hanson, D. C.; Jiang, Z. Q.; Lee, K. J.; Foote, C. S. *J. Am. Chem. Soc.* **1984**, *106*, 4570−4575. (b) Fukuzumi, S.; Fujita, S.; Suenobu, T.; Yamada, H.; Imahori, H.; Araki, Y.; Ito, O. *J. Phys. Chem. A* **2002**, *106*, 1241−1247.
(50) The maximum quantum yield for the formation of $(TBP_8Cz)Mn^V(O)$ was determined to be 0.028% for hexamethylbenzene (0.10 M).
(51) Kim, S. O.; Sastri, C. V.; Seo, M. S.; Kim, J.; Nam, W. *J. Am. Chem. Soc.* **2005**, *127*, 4178−4179.
(52) Tokumura, K.; Ozaki, T.; Nosaka, H.; Saigusa, Y.; Itoh, M. *J. Am. Chem. Soc.* **1991**, *113*, 4974−4980.
(53) A radical clock substrate (*trans*-1-methyl-2-phenylcyclopropane) with fast rearrangement (4×10^{11} s^{-1})[54] may be useful to confirm the oxygen rebound mechanism in Scheme 2. Appropriate radical clocks which have enough reactivity with $(TBP_8Cz)Mn^{IV}(O_2^{\bullet-})$ should be chosen to gain more insights into the lifetimes of substrate radicals in the rebound pathway for the future study.
(54) Atkinson, J. K.; Hollenberg, P. F.; Ingold, K. U.; Johnson, C. C.; Le Tadic, M.-H.; Newcomb, M.; Putt, D. A. *Biochemistry* **1994**, *33*, 10630−10637.
(55) (a) Parshall, G. W.; Ittel, S. D. *Homogeneous Catalysis*, 2nd ed.; Wiley: New York, 1992; Chapter 10. (b) Sheldon, R. A.; Kochi, J. K. *Adv. Catal.* **1976**, *25*, 272−413.
(56) (a) Kochi, J. K.; Krusic, P. J.; Eaton, D. R. *J. Am. Chem. Soc.* **1969**, *91*, 1877−1879. (b) Krusic, P. J.; Kochi, J. K. *J. Am. Chem. Soc.* **1968**, *90*, 7155−7157. (c) Krusic, P. J.; Kochi, J. K. *J. Am. Chem. Soc.* **1969**, *91*, 3938−3940. (d) Krusic, P. J.; Kochi, J. K. *J. Am. Chem. Soc.* **1969**, *91*, 3942−3944. (e) Kochi, J. K.; Krusic, P. J. *J. Am. Chem. Soc.* **1969**, *91*, 3944−3946. (f) Howard, J. A.; Furimsky, E. *Can. J. Chem.* **1974**, *52*, 555−556.
(57) (a) Fukuzumi, S.; Ono, Y. *J. Chem. Soc., Perkin Trans. 2* **1977**, 622−625. (b) Fukuzumi, S.; Ono, Y. *J. Chem. Soc., Perkin Trans. 2* **1977**, 625−630. (c) Hendry, D. G. *J. Am. Chem. Soc.* **1967**, *89*, 5433−5438. (d) Zwolenik, J. J. *J. Phys. Chem.* **1967**, *71*, 2464−2469. (e) Bennett, J. E.; Brown, D. M.; Mile, B. *Trans. Faraday Soc.* **1970**, *68*, 397−405.
(58) The concentration of cumylperoxyl radical generated in an EPR tube under photoirradiation is $\sim 10^{-6}$ M calculated by the integration of EPR spectrum.
(59) (a) Fukuzumi, S.; Ohkubo, K.; Suenobu, T.; Kato, K.; Fujitsuka, M.; Ito, O. *J. Am. Chem. Soc.* **2001**, *123*, 8459−8467. (b) Murakami, M.; Ohkubo, K.; Fukuzumi, S. *Chem.—Eur. J.* **2010**, *16*, 7820−7832.
(60) Mayer, J. M. *Acc. Chem. Res.* **1998**, *31*, 441−450.
(61) Wu, Y.-D.; Wong, C.-L.; Chan, K. W. K. *J. Org. Chem.* **1996**, *61*, 746−750.
(62) (a) Wagner, P. J.; Lam, H. M. H. *J. Am. Chem. Soc.* **1980**, *102*, 4167−4172. (b) Matsushita, Y.; Yamaguchi, Y.; Hikida, T. *Chem. Phys.* **1996**, *213*, 413−419.
(63) Fukuzumi, S.; Ohkubo, K. *J. Am. Chem. Soc.* **2002**, *124*, 10270−10271.
(64) The KIE value is somewhat larger than those observed for proton-transfer reactions of $AcrH_2^{\bullet+}$ (KIE = 9−10) probably because of a larger contribution of the tunneling effect. See: (a) Fukuzumi, S.; Tokuda, Y.; Kitano, T.; Okamoto, T.; Otera, J. *J. Am. Chem. Soc.* **1993**, *115*, 8960−8968. (b) Ishikawa, M.; Fukuzumi, S. *J. Chem. Soc., Faraday Trans. 1* **1990**, *86*, 3531−3536. (c) Fukuzumi, S.; Koumitsu, S.; Hironaka, K.; Tanaka, T. *J. Am. Chem. Soc.* **1987**, *109*, 305−316.